


 Cite this: *RSC Adv.*, 2022, **12**, 18585

# Fabrication of robust silver plated conductive polyamide fibres based on tannic acid modification

 Xin Ai,<sup>ab</sup> Jin Cheng,<sup>ab</sup> Xueni Hou,<sup>\*ab</sup> Guoqiang Chen<sup>ID</sup><sup>ab</sup> and Tieling Xing<sup>ID</sup><sup>\*ab</sup>

A novel method for the preparation of silver plated conductive polyamide fibres (PA/Ag) based on tannic acid modification was reported in this work. The highly adhesive tannic acid was grafted onto the surface of sulphuric acid roughened polyamide fibres to sensitize the fibre. Then, the sensitized polyamide fibres were activated by low-concentration silver nitrate to form reactive centers. Chemical silver plating was finally carried out using silver ammonia solution with glucose. The surface morphology and chemical properties of the prepared polyamide fibres were analyzed and the surface resistance, fastness to washing, thermal decomposition properties, electrothermal properties, sensing properties and practical applications of the silver-plated polyamide fibres were also tested. The test results show that the prepared conductive fibres have excellent conductivity and stability, and have potential applications in flexible electronic devices and sensing fields.

 Received 17th May 2022  
 Accepted 19th June 2022

DOI: 10.1039/d2ra03116g

[rsc.li/rsc-advances](http://rsc.li/rsc-advances)

## 1 Introduction

Polyamide (PA) fibre, also known as nylon, is an aliphatic polyamide connected by amide bond.<sup>1</sup> The  $-\text{CH}_2-$  in the polyamide molecules can generate weak van der Waals forces, and the  $\text{C}=\text{O}$  and  $-\text{NH}-$  groups contained in the molecules can form hydrogen bonds between or within molecules to form an excellent crystalline structure.<sup>2</sup> Therefore, polyamide fibre has a wide range of applications because of its excellent mechanical properties, wear resistance and corrosion resistance. However, polyamide fibre easily undergoes static charge accumulation, which brings many disasters to production and processing,<sup>3,4</sup> and has a negative impact on daily life. Therefore, it is necessary to modify the conductivity of polyamide fibre.

There are three main preparation methods of conductive fabric. The first one is metallization of the fabric surface.<sup>5</sup> A layer of metal is coated on the fabric surface by magnetron sputtering,<sup>6</sup> electroless plating<sup>7</sup> and evaporation spin coating.<sup>8</sup> The commonly used metals include silver, nickel and copper. The second method: conductive polymers like polyaniline<sup>9</sup> or polythiophene<sup>10</sup> are compounded with the fabric through special processes such as coating and penetration to give the fabric conductivity. The third type: ordinary fiber and metal fiber are mixed to form conductive fabric.<sup>11</sup>

Among the conductive treatments for fibres, electroless plating is the most effective,<sup>12</sup> high utilization, simple operation and relatively low cost. Silver is the most widely used metallic

layer in electroplating materials,<sup>13,14</sup> which is dense and uniform, without obvious defects and high bonding strength.<sup>15,16</sup> Therefore, electroless silver plating was carried out by silver mirror reaction between silver nitrate solution and glucose after sensitization and activation treatment.

Polyamide fibres can be etched under acidic conditions to form surface pits, which can expose reactive groups such as amino and carboxyl groups, so as to greatly increase the surface activity of the fibres and provide more attachment sites for subsequent reactions. In this work, sulphuric acid was used to roughen the polyamide fibres.

Tannic acid (TA) is a kind of polyphenol compound and secondary organism produced by plant metabolism in the process of plant growth, which is rich in natural resources, mainly in gallnut. TA is easily oxidized to quinones under weak alkaline conditions, which can graft to the fibre surface through Michael addition and Schiff base reactions with amino groups on the surface of roughened polyamide fibres.<sup>17</sup> The oxidative polymerization of dopamine for the functional modification of textile fibers has drawn great attention.<sup>18,19</sup> Moreover, reducing tannic acid grafted on the polyamide fibres can be used as the sensitizer, which can replace the skin irritant stannous chloride commonly used in fibre sensitization.<sup>20</sup> In addition, tannic acid contains a large number of highly adhesive catechol groups, which can complex silver ions,<sup>21</sup> and can greatly improved the fastness, denseness and surface uniformity of the plated fibres.

In this study, a simple and highly efficient method was used to modify the surface of inert polyamide fibres. Firstly, the fibres were roughened with sulphuric acid to provide more reaction sites and reactive groups, then sodium perborate was used to induce the grafting of reducing tannic acid with polyamide fibres. A layer of dense tannic acid was coated on the rough

<sup>a</sup>College of Textile and Clothing Engineering, Soochow University, Suzhou 215123, China. E-mail: xingtailing@suda.edu.cn; houxueni@suda.edu.cn

<sup>b</sup>Jiangsu Engineering Research Center of Textile Dyeing and Printing for Energy Conservation, Discharge Reduction and Cleaner Production (ERC), Soochow University, Suzhou 215123, China



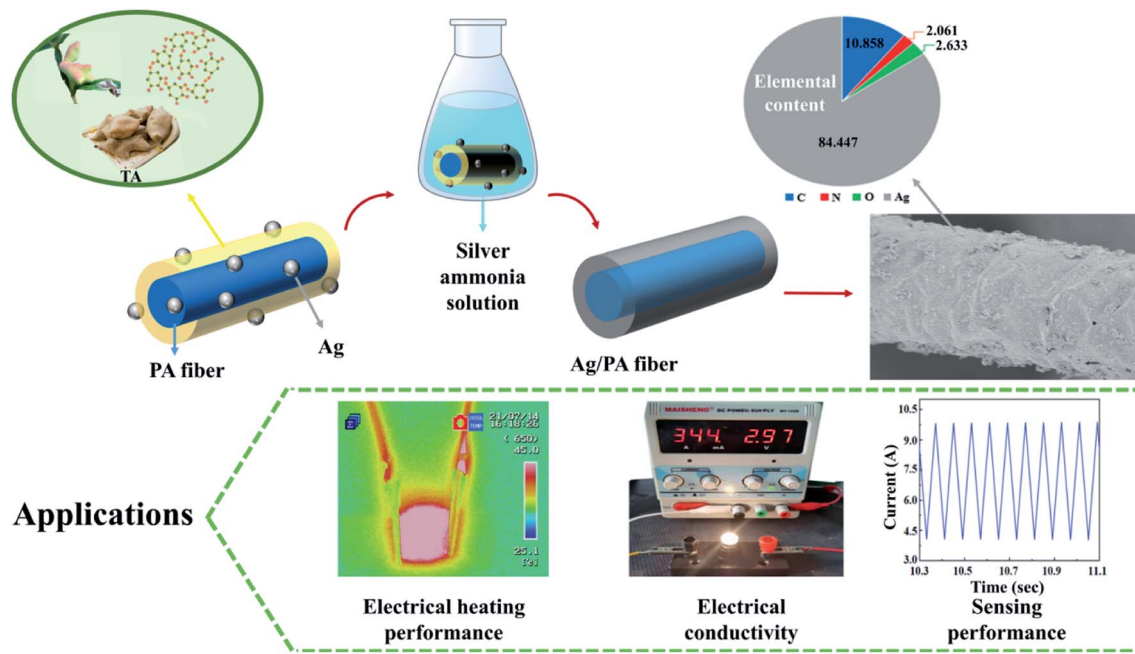


Fig. 1 Schematic of preparation of Ag/PA fibres (the statistical chart shows the element composition of the Ag/PA fibre surface).

nylon fibres, and the high adhesion of tannic acid was used as sensitizer. Silver nitrate was then used to activate the polyamide fibres to form reactive centers, and a uniform and dense silver layer was coated on the outermost layer of the fibres through silver mirror reaction. The conductive polyamide fibres (PA/Ag) were successfully prepared by using the excellent electrical conductivity of silver. The surface morphology of the prepared conductive polyamide fibres were observed by SEM, the chemical elements and structure of fibres were characterized by XRD and XPS. The conductivity, strength of the fibres, soaping fastness, stability of thermal decomposition, electrothermal performance, sensing performance and small light bulb luminescence experiments were carried out. Fig. 1 shows the schematic of preparation of Ag/PA fibres.

## 2 Experimental

### 2.1 Materials

Polyamide knitted fabric ( $50 \text{ g m}^{-2}$ , single fibre diameter  $20 \mu\text{m}$ ) was supplied by Suzhou Teck Silver Fibre Technology Co., Ltd. Tannic acid was purchased from Shanghai Yuanye Biotechnology Co., Ltd. Sulfuric acid, sodium perborate and silver nitrate were of analytical reagent grade and used without further purification.

### 2.2 Preparation of PA/Ag conductive fibres

The preparation of PA/Ag conductive fibres includes four main stages: roughening of fabric, grafting of oxidized tannic acid on the surface of the fabric, sensitization of fabric with low concentration of silver nitrate and silver plating on polyamide fabric surface. Fig. 2 shows the preparation process of Ag/PA fibres.

**2.2.1 Roughening of polyamide fabrics.** The polyamide fabric was first cleaned and oil removed, soaked in  $4 \text{ mol L}^{-1}$  sulfuric acid at  $25 \text{ }^\circ\text{C}$  for 1 minute, then cleaned and dried with hot air, and thoroughly dried to obtain roughened polyamide fabric.

**2.2.2 Sensitization of polyamide fabric surface by tannic acid.** First, the mixed solution of sodium perborate and tannic acid was prepared, and the roughened polyamide fabric was immersed into the mixed solution, so that tannic acid can be fully oxidized and grafted to the surface of fabric. Then the fabric was taken out and dried with hot air to obtain sensitized polyamide fabric.

**2.2.3 Activation of polyamide fabric surface by low concentration silver nitrate.** A low concentration silver nitrate solution was prepared and the tannic acid sensitized fabric was soaked at room temperature to form a large number of reaction sites on the fabric surface, then the fabric was taken out and dried with hot air.

**2.2.4 Silver plating on the surface of polyamide fabric.** Freshly prepared silver ammonia solution was used to electroless plate the fabric and magnetically stirred at 120 rpm at room temperature. After taking out and cleaning, the fabric was dried with hot air. Thus, polyamide fibres with silver plating on the surface were obtained.

### 2.3 Characterization

The element content of samples at each treatment stage was analyzed by benchtop scanning electron microscope (TM3030) at a scanning current of 5.0 kV. A Hitachi S-4800 scanning electron microscope was utilized to observe the surface morphology of the treated fibres at each stage under 3 kV accelerating voltage. The crystal structure of the fibres was analyzed using an X-ray diffractometer (XRD Smartlab) using



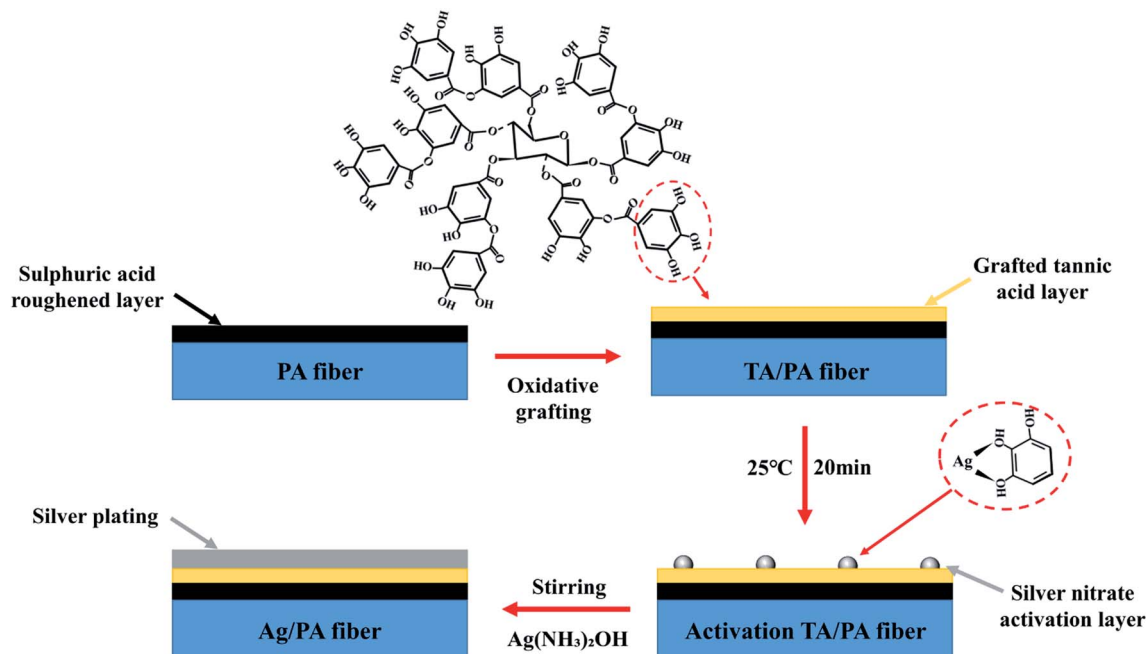


Fig. 2 Preparation process of Ag/PA fibres.

a copper target at a wavelength of 0.154 nm and a diffraction angle in the range  $0^\circ$ – $90^\circ$ . X-ray photoelectron spectroscopy (XPS) of the fibres was examined using a Thermo ESCALAB 250XI (Thermo Fisher Scientific, USA) in the binding energy test range of 200–800 eV, high performance data acquisition at low power (72 W) using a microfocal monochromatic source with full spectral scan (flux energy 100 eV in 1 eV steps); narrow spectral scan (flux energy 30–50 eV in 0.05–0.1 eV steps). Colorimeter for textile colour characteristics (Hunter lab) was used to characterize the color depth of fabric after tannic acid grafting and silver nitrate activation under 350 nm of wavelength at 25 °C and a relative humidity of 65%.

## 2.4 Stability tests

**2.4.1 Mechanical stability test.** Prior to testing, five samples were randomly selected from each batch and placed in a constant temperature and humidity chamber for 24 hours. The tensile strength of polyamide fibres was tested using an INSTRON-3365 material testing machine (INSTRON Corporation, Norwood, MA, USA) with 0.1 cN dex<sup>-1</sup> of pre-tension, 2 cm of clamping length and 10 cm min<sup>-1</sup> tensile speed. The data were recorded and the mean and variance were calculated.

**2.4.2 Soaping stability test.** According to the test method of AATCC 61-2006, TSA008 washing resistance tester was used to test the washing resistance of the fibres. The fibres were put into the tester with 1 : 50 ratio of soaping solution and rotated above 30 rpm at 40 °C for 30 min, which was repeated 8 times (equivalent to 40 times of washing with ordinary soap in tap water). After soaping and drying, the fastness of silver plating on the fibre surface was statistically analyzed by measuring the fibre electric resistance and the change in fibre resistance under different soaping times.

**2.4.3 Thermal stability analysis.** The sample fibres were cut into powder and the initial sample weight was controlled between 5 mg and 10 mg. Thermogravimetric analysis was carried out using a 2960 SDT 290 TA instrument at a temperature range of 30–600 °C, a heating rate of 20 °C min<sup>-1</sup> and an air flow rate of 100 mL min<sup>-1</sup>.

## 2.5 Electrical conductivity test

The electrical conductivity of PA/PEDOT conductive fibre was tested using a handheld multimeter (F15B+/F17B). The test length was one centimetre and five fibres were taken from the same batch of samples and each fibre was tested in three different locations. The data were recorded and the average and variance were calculated.

## 2.6 Electrothermal performance test

The surface of the prepared PA/Ag knitted fabric was heated within 120 seconds at an ambient temperature of 26.8 °C, a constant voltage of 15 V and a constant current of 0.1 A. A SZT-C type rapid constant voltage test bench (Suzhou Jingle Electronics Co., Ltd) was used to output constant voltage. An infrared thermometer (DT-810) was applied to measure the real time temperature of fibre surface over a fixed distance of five centimetres, and a FOTRIC 800 thermal infrared imager was used to take thermal infrared image of fibres at 25–45 °C (measuring distance of 15 cm).

## 2.7 Sensing performance tests

The internal resistance and the resistance change rate over time of PA/Ag fibres with length of 5 cm were measured using AUTOLAB PGSTAT302 electrochemical workstation due to the



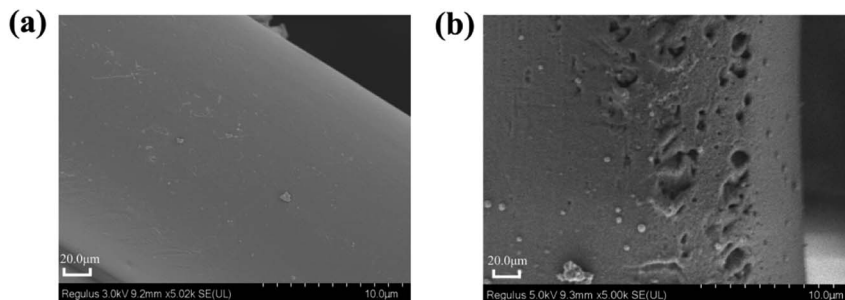


Fig. 3 SEM image of original polyamide fibre (a); polyamide fibre after sulfuric acid roughening (b).

deformation of the fibres under external forces such as bending and compression.

### 2.8 LED lamp test

A simple circuit consisting of PA/Ag fibre, which was placed in a constant temperature and humidity room for more than 24 hours, a small LED lamp, a SZT-C type rapid constant voltage test bench and wires. The voltage was then adjusted to observe the change in brightness of the lamp and the change in the current value in the circuit at different voltages.

## 3 Results and discussion

### 3.1 Roughening of the fibre surface

The pretreatment of polyamide fibre is of great importance, especially in fibre modification, which can directly affect the subsequent treatment effect.<sup>22</sup> In this study, sulphuric acid treatment was used to form pits on the surface of polyamide fibres, exposing more reactive groups without destroying the internal structure of the fibres. The surface morphology of polyamide fibre before and after roughening can be observed by SEM. Fig. 3(a) indicates that the surface of the original polyamide fibre is flat and smooth. Fig. 3(b) shows that pits appear on the surface of polyamide fibre treated with sulfuric acid.

### 3.2 Sensitization conditions for polyamide fibres

Different from the conventional sensitization of fibres using stannous chloride,<sup>23</sup> the fibre sensitization in this study was carried out by oxidative grafting of tannic acid on the fibre surface. After grafting of tannic acid on the fibre surface, a highly adhesive film can be established on the polyamide fibre surface to facilitate the subsequent reaction. The oxidative grafting is mainly influenced by the reaction temperature, oxidation time, pH value and the concentration of tannic acid and oxidant,<sup>24</sup> among which the concentration of tannic acid and oxidant is the main influencing factor. Fig. 4(a) shows the SEM image of the polyamide fibre after oxidative grafting with tannic acid, in which a dense layer of tannic acid is grafted on the fibre surface. Fig. 4(b) shows the color depth of the polyamide fabric at 350 nm for different ratios of tannic acid and oxidizing agent at 75 °C, pH 8 and 2 hours reaction time. It is obviously that the color depth gradually increased with the increase of the ratio, and the increasing trend became

significantly slower after the molar mass ratio was 2 : 1. In order to increase the utilization of the chemicals and eliminate waste, the molar mass ratio of tannic acid to oxidant was selected as 2 : 1.

### 3.3 Activation conditions of low concentration silver nitrate

Fig. 4(c) shows the SEM image of the polyamide fabric activated by silver nitrate. It can be seen that there are many silver particles on the surface of the fabric facilitating the deposition of a large number of silver ions in the subsequent silver plating process, which can greatly improve the utilization rate of silver nitrate and reduce the loss of chemicals and hence the cost. Fig. 4(d) shows the color depth of the polyamide fabric at 350 nm treated with different concentrations of silver nitrate solution at 75 °C, pH 8 and reaction time of 2 hours. It can be seen that the fabric color depth increases with the increase of silver nitrate concentration until the concentration of  $4 \times 10^{-5} \text{ mol L}^{-1}$ , after which the curve becomes almost flat. Considering the cost and utilization of silver nitrate,  $4 \times$

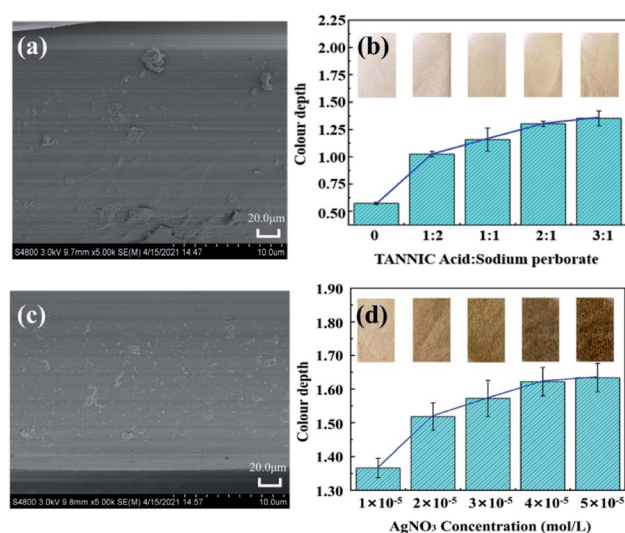


Fig. 4 SEM images of PA fabric after tannic acid sensitization (a); changes in color depth of fabric after sensitization with different tannic acid concentrations (b); fabric activated with low concentrations of silver nitrate (c); changes in color depth of fabric after activation with different concentrations of silver nitrate (d).



$10^{-5}$  mol L<sup>-1</sup> silver nitrate was chosen as the optimum concentration for this study.

### 3.4 Analysis of the surface morphology and chemical structure composition of PA/Ag fibres

**3.4.1 SEM and EDS.** Fig. 5(a) shows the SEM image of the surface of the original polyamide fibre, which is smooth and flat. Fig. 5(b)–(d) show the SEM images of the surface of PA/Ag fibres prepared under optimal conditions with a 1500 $\times$ , 3000 $\times$  and 20 000 $\times$ , respectively. A dense and homogeneous layer of monolithic silver distributes on the surface of the lower magnification SEM image, and granular monolithic silver particles can be seen on the surface of the fibres at higher magnification SEM image. Fig. 5(e)–(h) show the distribution of elemental content at each treatment stage, and it can be observed that the original polyamide fibres contain three main elements, C, N and O.<sup>25</sup> After the sulphuric acid roughening treatment, although the surface roughness increased, the elemental species did not change, but the relative content of individual elements.<sup>26</sup> After sensitization with tannic acid and silver nitrate activation, about 20% of silver elements appeared on the surface of the fibres, and the silver content on the surface of the fibres after silver plating was up to more than 84%, indicating that the surface of the fibres was covered with a dense layer of silver.

**3.4.2 XRD and XPS analysis.** Fig. 6(a) shows the XRD patterns of the original polyamide fibres, tannic acid treated fibres and the PA/Ag fibres. It is obvious from the figure that the two diffraction peaks of the original polyamide fibres are located at 21.5 $^{\circ}$  and 23.9 $^{\circ}$ , respectively.<sup>27</sup> The tannic acid treatment had little effect on the crystallinity of the fibres, so the peak positions and the crystalline intensity of the tannic acid

treated fibres were almost unchanged compared with the original polyamide fibres. After the silver plating treatment, the silver plating can cover the original diffraction peaks of the polyamide fibres due to the crystallinity of silver. Therefore, there were clear diffraction peaks on the crystalline surface of silver plating layer, which are located at 38.2 $^{\circ}$ , 44.4 $^{\circ}$ , 64.6 $^{\circ}$  and 77.6 $^{\circ}$ ,<sup>28</sup> indicating that the fibres were covered with dense silver.

Fig. 6(b) and (c) shows the XPS wide scan and Ag<sub>3d</sub> spectrum of PA/Ag fibres prepared under the optimum process, respectively. The characteristic peaks of silver near Ag<sub>3d</sub> 5/2 (367 eV), Ag<sub>3d</sub> 3/2 (374 eV) and Ag<sub>3p</sub> 3/2 (574 eV), Ag<sub>3p</sub> 1/2 (606 eV) and Ag<sub>3s</sub> (718 eV) can prove that elemental silver on the surface of the fibres is singlet silver.<sup>29,30</sup>

### 3.5 Stability tests

Fig. 7(a) shows the strength of PA fibres at various stages of preparation. The strength of fibres changed from 386 cN cm<sup>-1</sup> of original fibres to 344 cN cm<sup>-1</sup> of PA/Ag fibres, and the strength approximately decreased by 10.9%, which did not affect the normal processing and use. In this process, the first part of the strength decline is the sulfuric acid roughening stage, which is caused by the acid intolerance of the polyamide fibres. The second stage of strength reduction is due to the addition of the oxidizing agent sodium perborate during the oxidative grafting of tannic acid, which has a definite impact on the strength of the fibres. The third stage of strength reduction is the silver plating process, which is mainly due to the oxidation of silver ammonia solution to the fibres.

Fig. 7(b) shows the changes in resistance of the prepared PA/Ag fibres after different times of washing. It can be seen that after 2 times of soaping (equivalent to 10 times of ordinary soaping), the resistance of the fibre tends to be stable and

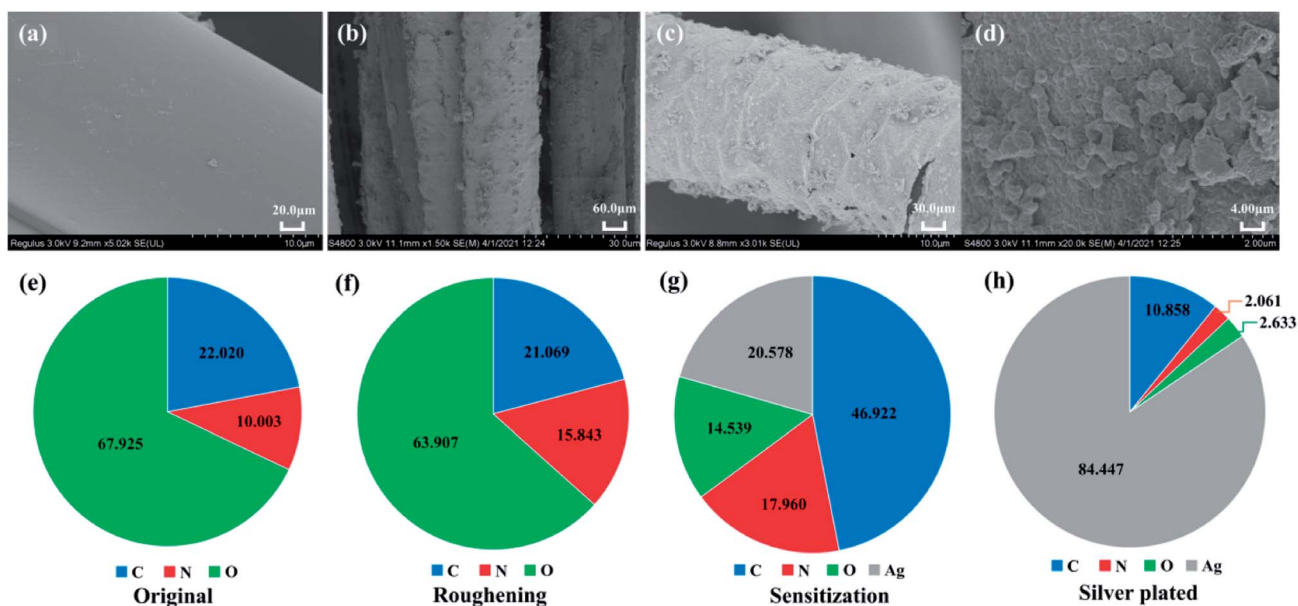


Fig. 5 SEM images of original polyamide fibre (a); the surface of PA/Ag fibres prepared under optimal conditions at 1500 $\times$  (b), 3000 $\times$  SEM image (c) and 20 000 $\times$  (d); elemental content distribution of untreated fibres (e); after sulphuric acid roughening (f); after tannic acid sensitization and silver nitrate activation (g); after silver plating (h).



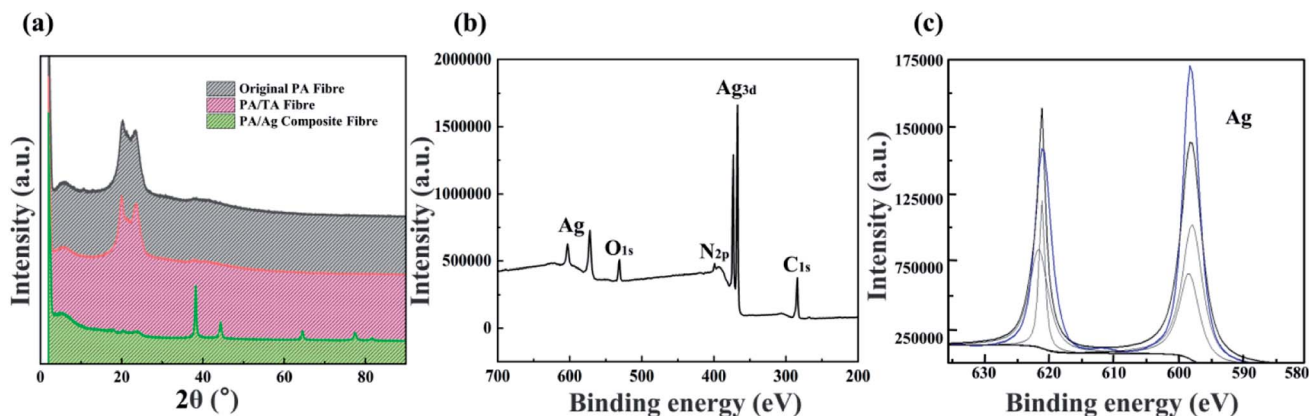


Fig. 6 XRD patterns of original polyamide fibres, tannic acid treated fibres and silver plated polyamide fibres (a); the XPS wide scan (b) and Ag<sub>3d</sub> spectrum (c) of PA/Ag fibres.

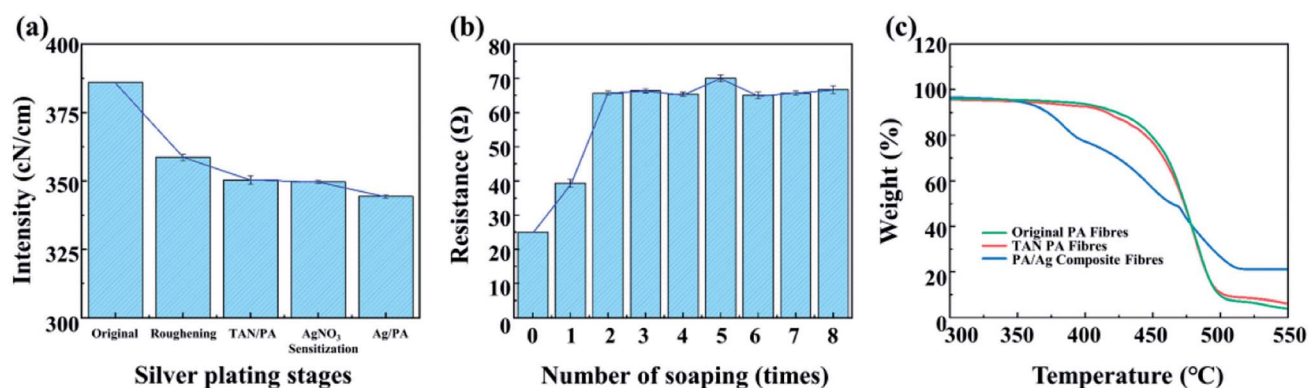


Fig. 7 Stability of PA/Ag fibres at various stages in strength (a) in resistance size of PA/Ag fibres after different number of washes (b); TG curves of PA, TAN/PA and PA/Ag fibres (c).

eventually stabilizes between 65  $\Omega$  and 75  $\Omega$ . The resistance becomes 2.8 times of the fibre before washing, and still maintains excellent electrical conductivity. Fig. 7(c) shows the TG curves of PA fibres, PA/TA fibres and PA/Ag fibres. From the change trend, it is obvious that the thermal weight loss process of the original PA fibres as well as the tannic acid treated fibres can be mainly divided into four stages: between 30 and 335  $^{\circ}\text{C}$ , the weight of fibres decrease slightly due to the evaporation of water in fibres, and the thermal weight loss does not change significantly; between 335 and 420  $^{\circ}\text{C}$ , the weight loss starts to increase, the weight loss rate of both the original PA fibre and the tannic acid treated fibre is about 7.3%, while the weight loss of silver-plated fibre has a significant decrease at this stage; 421–480  $^{\circ}\text{C}$  is the third stage, in which the weight loss rate is the largest. The weight loss of the original fibre and the tannic acid treated fibre is basically the same, and the weight loss of silver-plated fibre decrease slightly with the increase in temperature. The final stage of the thermal analysis is after 480  $^{\circ}\text{C}$ , in which the fibre residue is further burnt out to complete carbonization. The experimental data show that the silver-plated polyamide fibres have good thermal decomposition stability and can be used in high temperature environment.

### 3.6 Factors influencing the resistance of PA/Ag fibres

Fig. 8 shows the effects of different silver plating pH (a), time (b) and silver nitrate concentration (c) on the electrical conductivity of silver plated fibres. As shown in Fig. 8(a), it is clear that the silver plating effect is excellent under neutral or weak alkaline conditions, while keeping other influencing factors constant. The silver ammonia solution itself is weakly alkaline,<sup>31</sup> so there is no need to adjust the solution pH during use. As can be seen from Fig. 8(b), before 25 min of plating time, the longer the time, the better the compactness and thickness of the silver layer, so the electrical conductivity gradually increased; after 25 min, due to the continuous redox reaction in the plating solution, the reduced singlet silver accumulates on the surface of the fibres and the thickness of the silver layer increases, which leads to the decrease of washing fastness, so the resistance begins to increase slightly. Fig. 8(c) shows the effect of silver nitrate concentration on the electrical conductivity of the fibres. Silver nitrate, as the main salt, provides silver ions for the whole reaction and direct affects the electrical conductivity. Keeping other influencing factors constant, the electrical conductivity increases significantly with the increase of silver ion concentration until the concentration of silver nitrate is 3 g



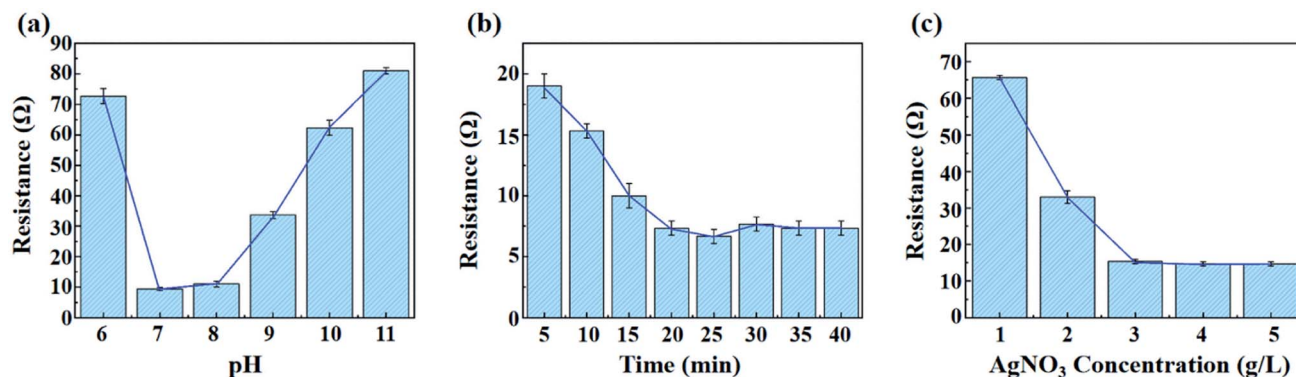


Fig. 8 Effects of silver plating pH (a); plating time (b) and silver nitrate concentration (c) on resistance.

$L^{-1}$ . After this concentration, the change of fibre conductivity is not significant with the increase of silver nitrate. Considering various factors such as cost, utilization and metal pollution,<sup>32</sup>  $3 \text{ g L}^{-1}$  silver nitrate was used for silver plating in this study.

Therefore, the conductivity of the fibre is achieved when plated with  $3 \text{ g L}^{-1}$  silver nitrate for 20–25 min under weak alkaline condition.

## 4 Practical applications of PA/Ag fibres

### 4.1 Electro-thermal performance

Fig. 9(a) shows the experimental model of the electrothermal performance of PA/Ag fibres knitted fabric. Fig. 9(b)–(h) show the thermal infrared images of PA/Ag fibres knitted fabric with the size of  $2 \text{ cm} \times 1 \text{ cm}$  at  $25\text{--}45^\circ\text{C}$  under the condition of constant  $2.5 \text{ V}$  and  $2 \text{ A}$  using FOTRIC 800 thermal infrared imager within 0–30 s after power on at  $27.7^\circ\text{C}$  of ambient temperature. Fig. 9(i) shows the temperature–time curve under the same conditions. It can be seen that with the increase of time, the surface temperature of the fibres rises rapidly in a short time, especially in the first 10 seconds, the temperature rises significantly from  $27.7^\circ\text{C}$  at the beginning to  $32.6^\circ\text{C}$ . After 10 seconds, the growth rate of

the temperature tends to be gentle and basically stable after 20 seconds. According to the thermal infrared imaging, it is obvious that the temperature of the knitted fabric rises significantly after energisation, which indicates that PA/Ag fibres have excellent electrothermal conversion performance and have great development prospects in the field of heating health care products as well as heat generating fabrics.<sup>33</sup>

### 4.2 Sensing and conductivity

Fig. 10(a) shows the physical model diagram of PA/Ag fibres in constant repetitive motion from the straightened state to the bent state, and Fig. 10(b) shows the change in current with time generated in the repetitive bent and straightened state. It can be seen that the current can change rapidly in short time when the fibres are deformed, indicating that PA/Ag fibres can transform the mechanical signals into electrical signals in time. Therefore, the fibres can be used to prepare wearable sensors and sensing garments<sup>34</sup> for motion posture and expression monitoring, smart sensing garments and other fields.<sup>35</sup> Fig. 10(c) shows the experimental model of a small bulb emitting light, and Fig. 10(d) shows a brighter light at  $2 \text{ V}$  of voltage and  $0.28 \text{ A}$  of circuit current. Fig. 10(e) shows the small bulb emitting a dazzling light at  $3 \text{ V}$  of voltage and  $0.34 \text{ A}$  of circuit current. It

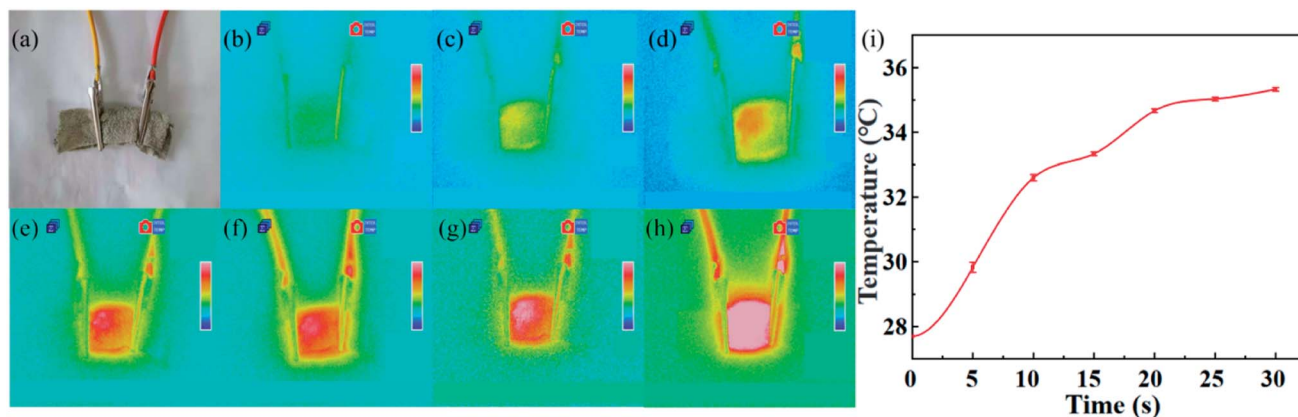


Fig. 9 Experimental model of the electrothermal properties of PA/Ag fibre knitted fabrics (a); infrared thermography of fibres no power (b); within 5 s of energisation (c); within 10 s of energisation (d); within 15 s of energisation (e); within 20 s of energisation (f); within 25 s of energisation (g); within 30 s of energisation (h); temperature–time curve after power on (i).



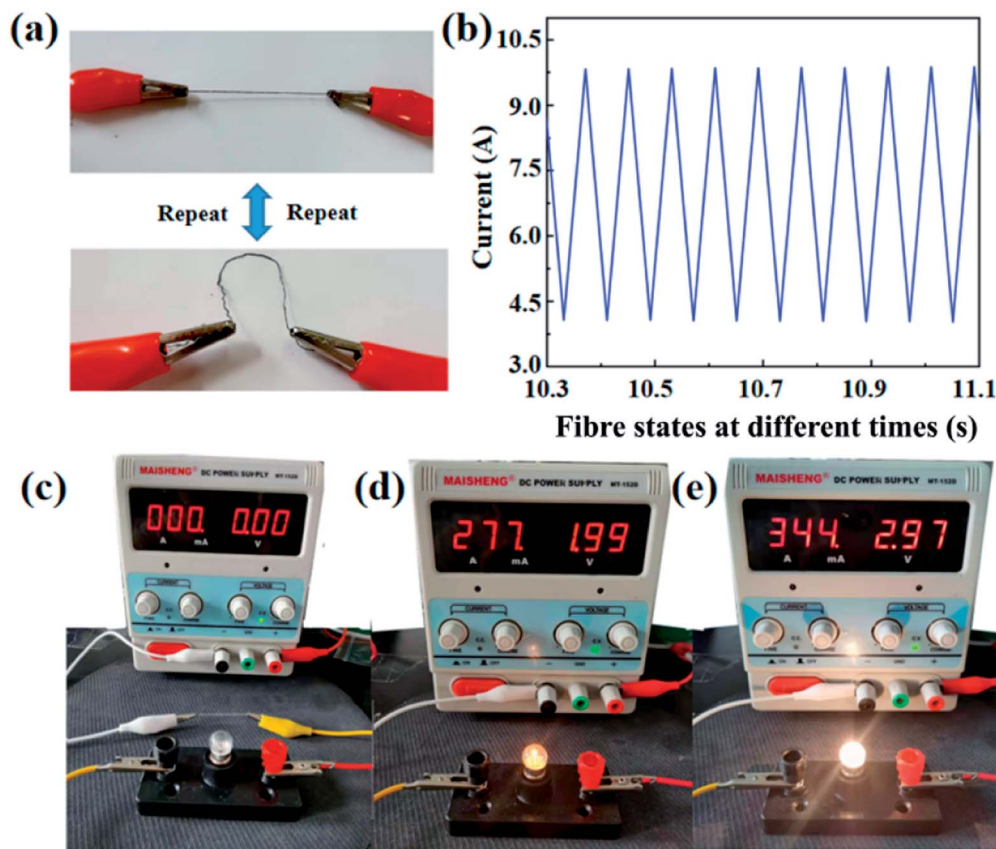


Fig. 10 PA/Ag fibres in straightened state and bent state (a); current–time curve under repeated bending and straightening (b); experimental model of a small light bulb luminescence test (c); the light emitted by a small bulb at a voltage of 2 V and a circuit current of 0.28 A (d); the light emitted from a small bulb at a voltage of 3 V and a circuit current of 0.34 A (e).

can therefore be demonstrated that PA/Ag conductive polyamide fibres have good conductive properties and can be used as an e-textile in LED power supply circuit.<sup>36</sup>

## 5 Conclusion

In this study, an environmentally friendly preparation method was provided to fabricate PA/Ag conductive fibres by oxidatively grafting natural polyphenols onto polyamide fibres for sensitization and activating the fibre surface with a low concentration of silver nitrate to enhance the reactivity of the fibre surface, followed by a silver mirror reaction to form dense silver on the fibre surface. The prepared PA/Ag fibres have good electrical conductivity, mechanical and washing stability, and electro-thermal performance, which have promising applications in electronic textiles and heat-generating fabrics.

## Conflicts of interest

The authors state no conflicts of interest.

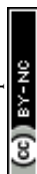
## Acknowledgements

This work was supported by the National Natural Science Foundation of China (Grant No. 51973144, 51741301), the Key R & D plan of Jiangsu Province (BE2019001) and the Foundation

of Jiangsu Engineering Research Center of Textile Dyeing and Printing for Energy Conservation, Discharge Reduction and Cleaner Production (Q811580621).

## References

- 1 K. K. Cao, Y. F. Liu, F. Yuan, Y. Yang, J. Wang, Z. C. Song, Z. L. Wu, M. J. Jiang and J. Yang, *High Perform. Polym.*, 2021, **33**, 1083–1092, DOI: [10.1177/09540083211020814](https://doi.org/10.1177/09540083211020814).
- 2 X. H. Kuang, J. P. Guan, R. C. Tang and G. O. Chen, *Mater. Res. Express*, 2017, **4**, 095302, DOI: [10.1088/2053-1591/aa7fc6](https://doi.org/10.1088/2053-1591/aa7fc6).
- 3 T. Xu and H. Xie, *Advances in Engineering Research*, 2015, **12**, 683–686.
- 4 L. P. Wang, J. Y. Gao, Z. G. Gao, L. L. Wu and C. A. Ge, *Text. Bieng. Inf. Symp., Proc., 11th*, 2010, 750–753, DOI: [10.3993/tbis2010131](https://doi.org/10.3993/tbis2010131).
- 5 M. Grell, C. Dincer, T. Le, A. Lauri, E. N. Bajo, M. Kasimatis, G. Barandun, S. A. Maier, A. E. G. Cass and F. Guder, *Adv. Funct. Mater.*, 2019, **29**, 1804798, DOI: [10.1002/adfm.201804798](https://doi.org/10.1002/adfm.201804798).
- 6 C. L. Chu, X. F. Hu, H. Q. Yan and Y. Y. Sun, *e-Polymers*, 2021, **21**, 140–150, DOI: [10.1515/epoly-2021-0020](https://doi.org/10.1515/epoly-2021-0020).
- 7 L. B. Li, L. Wang, L. Wang and B. Liu, *Rare Met. Mater. Eng.*, 2010, **39**, 20–23.



- 8 U. Akin, O. F. Yuksel and N. Tugluoglu, *Silicon*, 2021, **14**, 2201–2209, DOI: [10.1007/s12633-021-01017-3](https://doi.org/10.1007/s12633-021-01017-3).
- 9 Y. A. Yuan, Y. Y. Xiao, Z. X. Jia, L. Y. Li, D. L. Sun, H. F. Zhang, N. Tang and X. C. Wang, *J. Nat. Fibers*, 2020, **17**, 1479–1487, DOI: [10.1080/15440478.2019.1579691](https://doi.org/10.1080/15440478.2019.1579691).
- 10 Y. R. Wang, X. Ai, S. Z. Lu, T. L. Xing, N. Qi and G. Q. Chen, *Colloids Surf., A*, 2021, **625**, 126909, DOI: [10.1016/j.colsurfa.2021.126909](https://doi.org/10.1016/j.colsurfa.2021.126909).
- 11 Y. Lu, J. W. Jiang, S. Park, D. Wang, L. H. Piao and J. Kim, *Bull. Korean Chem. Soc.*, 2020, **41**, 162–169, DOI: [10.1002/bkcs.11945](https://doi.org/10.1002/bkcs.11945).
- 12 E. Magnone, S. H. Lee and J. H. Park, *Mater. Lett.*, 2020, **272**, 127811, DOI: [10.1016/j.matlet.2020.127811](https://doi.org/10.1016/j.matlet.2020.127811).
- 13 C. C. Liu, X. L. Li, X. Q. Li, T. Z. Xu, T. Z. Xu, C. Y. Song and Z. J. Gu, *Materials*, 2018, **18**, 2033, DOI: [10.3390/ma11102033](https://doi.org/10.3390/ma11102033).
- 14 C. C. Liu, J. Cheng, X. Q. Li, P. P. Yue, Z. J. Gu and K. J. Ogino, *J. Polym. Eng.*, 2019, **39**, 161–169, DOI: [10.1515/polyeng-2018-0205](https://doi.org/10.1515/polyeng-2018-0205).
- 15 Y. Mao, S. Q. Zhang, W. Wang and D. Yu, *Colloids Surf., A*, 2018, **558**, 538–547, DOI: [10.1016/j.colsurfa.2018.09.028](https://doi.org/10.1016/j.colsurfa.2018.09.028).
- 16 H. I. Lee, Y. J. Yim, K. M. Bae and S. J. Park, *Compos. Res.*, 2018, **31**, 76–81, DOI: [10.7234/composres.2018.31.2.076](https://doi.org/10.7234/composres.2018.31.2.076).
- 17 H. Y. Zhang, X. L. Li, H. B. Kang and X. Y. Peng, *Meat Sci.*, 2022, **188**, 108779, DOI: [10.1016/j.meatsci.2022.108779](https://doi.org/10.1016/j.meatsci.2022.108779).
- 18 X. H. Kuang, J. P. Guan, R. C. Tang and G. Q. Chen, *Mater. Res. Express*, 2017, **4**, 095302, DOI: [10.1088/2053-1591/aa7fc6](https://doi.org/10.1088/2053-1591/aa7fc6).
- 19 L. Jiang, Y. F. Zhou, Y. Guo, Z. Q. Jiang, S. J. Chen and J. W. Ma, *J. Appl. Polym. Sci.*, 2019, **136**, 47584, DOI: [10.1002/app.47584](https://doi.org/10.1002/app.47584).
- 20 S. Rapuntean, R. Balint, G. A. Paltinean, G. Tomoaia, A. Mocanu, C. P. Racz, O. Horovitz and C. Tomoaia, *Studia Universitatis Babeş-Bolyai. Chemia*, 2018, **63**, 73–85, DOI: [10.24193/subbchem.2018.3.06](https://doi.org/10.24193/subbchem.2018.3.06).
- 21 D. C. German, J. A. Garcia-Valenzuela, M. C. Leal, M. Martinez-Gil, R. Aceves and M. Sotelo-Lerma, *Mater. Sci. Semicond. Process.*, 2019, **89**, 131–142, DOI: [10.1016/j.mssp.2018.09.009](https://doi.org/10.1016/j.mssp.2018.09.009).
- 22 X. Chen, B. Q. Liu, D. Sheng, H. H. Xia, H. Pan, D. M. Wang, B. Deng and G. Y. Cao, *Text. Res. J.*, 2021, **91**, 1546–1554, DOI: [10.1177/0040517520985888](https://doi.org/10.1177/0040517520985888).
- 23 M. Lyapina, M. Dencheva, A. Krasteva, M. Cekova, M. Deliverska, V. Vodenicharov, D. Markov, Y. Mitova and A. Kisselova, *Biotechnol. Biotechnol. Equip.*, 2018, **32**, 707–713, DOI: [10.1080/13102818.2018.1450163](https://doi.org/10.1080/13102818.2018.1450163).
- 24 Y. J. Jing, Y. J. Diao and X. Q. Yu, *React. Funct. Polym.*, 2019, **135**, 16–22, DOI: [10.1016/j.reactfunctpolym.2018.12.005](https://doi.org/10.1016/j.reactfunctpolym.2018.12.005).
- 25 D. A. Lapkin, S. N. Malakhov, V. A. Demin, S. N. Chvalun and L. A. Feigin, *Synth. Met.*, 2019, **254**, 63–67, DOI: [10.1016/j.synthmet.2019.05.016](https://doi.org/10.1016/j.synthmet.2019.05.016).
- 26 E. B. Reed, S. Ard, J. La, C. Y. Park, L. Culligan, J. J. Fredberg, L. V. Smolyaninova, S. N. Orlov, B. H. Chen and R. Guzy, *Respir. Res.*, 2019, **20**, 168, DOI: [10.1186/s12931-019-1141-8](https://doi.org/10.1186/s12931-019-1141-8).
- 27 M. S. Kim, Y. N. Hwang, S. T. Kwon, S. G. Lee and H. H. Cho, *Fibers Polym.*, 2020, **21**, 2173–2178, DOI: [10.1007/s12221-020-9873-0](https://doi.org/10.1007/s12221-020-9873-0).
- 28 T. Raghavendra and K. Panneerselvam, *Fibers Polym.*, 2020, **21**, 2569–2578, DOI: [10.1007/s12221-020-9631-3](https://doi.org/10.1007/s12221-020-9631-3).
- 29 M. A. Saleem, L. J. Pei, M. F. Saleem, S. Shahid and J. P. Wang, *J. Cleaner Prod.*, 2020, **276**, 123258, DOI: [10.1016/j.jclepro.2020.123258](https://doi.org/10.1016/j.jclepro.2020.123258).
- 30 M. A. Saleem, L. J. Pei, M. F. Saleem, S. Shahid and J. P. Wang, *J. Cleaner Prod.*, 2020, **279**, 123480, DOI: [10.1016/j.jclepro.2020.123480](https://doi.org/10.1016/j.jclepro.2020.123480).
- 31 A. K. Tomer, T. Rahi, D. K. Neelam and P. K. Dadheech, *Int. Microbiol.*, 2019, **22**, 49–58, DOI: [10.1007/s10123-018-0026-x](https://doi.org/10.1007/s10123-018-0026-x).
- 32 I. J. Fernandes, A. F. Aroche, A. Schuck, P. Lamberty, C. R. Peter, W. Hasenkamp and T. L. A. C. Rocha, *Sci. Rep.*, 2020, **10**, 8878, DOI: [10.1038/s41598-020-65698-3](https://doi.org/10.1038/s41598-020-65698-3).
- 33 A. Kaynak, A. Zolfagharian, T. Featherby, M. Bodaghi, M. A. P. Mahmud and A. Z. Kouzani, *Materials*, 2021, **14**, 550, DOI: [10.3390/ma14030550](https://doi.org/10.3390/ma14030550).
- 34 S. M. Doshi, C. Murray, A. Chaudhari, D. H. Sung and E. T. Thostenson, *J. Mater. Chem. C*, 2022, **10**, 1617–1624, DOI: [10.1039/d1tc05132f](https://doi.org/10.1039/d1tc05132f).
- 35 Z. A. Abro, Y. F. Zhang, C. Y. Hong, R. A. Lakho and N. L. Chen, *Sens. Actuators, A*, 2018, **272**, 153, DOI: [10.1016/j.sna.2018.01.052](https://doi.org/10.1016/j.sna.2018.01.052).
- 36 A. Noda and H. Shinoda, *IEEE Access*, 2021, **9**, 69654, DOI: [10.1109/ACCESS.2021.3078133](https://doi.org/10.1109/ACCESS.2021.3078133).

